Online recognition of handwritten characters from scalp-recorded brain activities during handwriting

Leisi Pei, Guang Ouyang*

Faculty of Education, the University of Hong Kong, Pokfulam, Hong Kong SAR.

*Corresponding author, e-mail: ouyangg@hku.hk

Abstract

Objective: Brain-computer interfaces (BCI) aim to build an efficient communication with the world using neural signals, which may bring great benefits to human society, especially to people with physical impairments. To date, the ability to translate brain signals to effective communication outcome remains low. This work explores whether the handwriting process could serve as a potential interface with high performance. To this end, we first examined how much the scalp-recorded brain signals encode information related to handwriting and whether it is feasible to precisely retrieve the handwritten content solely from the scalp-recorded electrical data. *Approach:* Five participants were instructed to write the sentence "HELLO, WORLD!" repeatedly on a tablet while their brain signals were simultaneously recorded by electroencephalography (EEG). The EEG signals were first decomposed by independent component analysis for extracting features to be used to train a convolutional neural network (CNN) to recognize the written symbols. *Main results:* The accuracy of the CNN-based classifier trained and applied on the same participant (training and test data separated) ranged from 76.8 % to 97.0 %. The accuracy of cross-participant application was more diverse, ranging from 14.7 % to 58.7 %. These results showed the possibility of recognizing the handwritten content directly from the scalp level brain signal. A demonstration of the recognition system in an online mode was presented. The major factor that grounded the recognition was the close association between the rich dynamics of electroencephalogram source activities and the kinematic information during the handwriting movements. *Significance:* This work revealed an explicit and precise mapping between scalp-level electrophysiological signals and linguistic information conveyed by handwriting, which provided a novel approach to developing brain computer interfaces that focus on semantic communication.

1. Introduction

Brain-computer interfaces (BCI) have been undergoing rapid development in recent years with the leverage of advancing algorithms (Lotte et al., 2018). One of the major reasons driving this

field is that the development of BCI bears great significance in enhancing human's life by pushing the limits of communication and controlling efficiency between human and the world, and by enabling people with certain disabilities to regain some lost communication functions. Since language is the most important form of communication, many BCI systems have focused on building language production system based on brain signals. BCI speller is one example of this kind. In many previous applications, the signals to be translated to language outputs (e.g., a symbol) were usually perception-related neural signals. For example, the participants may be required to watch flicking letters that generate P300 or steady state visual evoked potentials (SSVEP) bound to the letters (Chen et al., 2015; Fazel-Rezai et al., 2012; Medina-Juliá, Fernández-Rodríguez, Velasco-Álvarez, & Ron-Angevin, 2020). These perception-based paradigms have demonstrated the possibilities but have not yet shown major breakthroughs in terms of practicality due to various reasons (e.g, perceptual fatigue, etc) (Zhang, Tan, Sun, Wu, & Zhang, 2018).

Another type of paradigm in the BCI field is imagery-based paradigm that uses internally generated neural information for controlling purposes. The majority of imagery-based paradigms is based on motor imaginary (MI), which has been less focused on language production but more on producing specific motor actions such as hand moving, reaching, and grasping (Aflalo et al., 2015; Alimardani, 2018; Padfield, Zabalza, Zhao, Masero, & Ren, 2019). Using motor imagery-based paradigm for language production has been rare in the applications that were based on scalp-level EEG. The low signal-to-noise ratio of scalp EEG may be the key reason because it imposes a great challenge in reading and transforming EEG data into efficient controlling signals with a practical utility (Abiri, Borhani, Sellers, Jiang, & Zhao, 2019; Rashid et al., 2020), despite the widely found associations between EEG and cognitive processes in the literature.

The scenario is remarkably different in signals directly recorded from the cortex by electrocorticography (ECoG). ECoG has the advantage of being less prone to artifacts and irreversible spatial mixing of different source activities (Buzsáki, Anastassiou, & Koch, 2012), it thus better retains the original forms of neural activities. Some remarkable recent advances have shown that ECoG signals recorded during speech production or perception can be used to synthesize the original speech, or be directly translated into text with an impressive accuracy (Angrick et al., 2019; Anumanchipalli, Chartier, & Chang, 2019; Makin, Moses, & Chang, 2020; Moses, Leonard, & Chang, 2018; Sun, Anumanchipalli, & Chang, 2020; Wilson et al., 2020). In addition, it has also been demonstrated that the ECoG signals during handwriting imagery can be decoded and used for typing purpose with a high performance (Willett,

Avansino, Hochberg, Henderson, & Shenoy, 2020). These works demonstrated a very clear mapping between the neural dynamics and the patterns of fine motor control activity. The mapping is most likely through the neural coding of detailed kinematic information of the actual or imagined motor activities (Anumanchipalli et al., 2019; Willett et al., 2020). Such a clear mapping is the foundation for BCI applications in the language domain.

However, although the above-mentioned breakthroughs in translating the brain signals to information in language forms are fascinating and important, the fact that they are based on cortex-level signals still places a major hurdle in the feasibility of their application in normal scenes. Therefore, it is important to explore the technological limits at the scalp (non-invasive) level for the purpose of achieving wide applications of language production BCI. To this end, the current work was dedicated to investigating the association between the scalp EEG and handwriting processes to lay a foundation for further development of scalp EEG-based BCI using the modality of handwriting. The major obstacle in this line lies in the low signal-to-noise ratio of the scalp level EEG—after its first discovery 100 years ago, there has not been groundbreaking advances in the accuracy of decoding mental activities based on scalp EEG, despite its extensively found association with various cognitive processes. Attempts to read the scalp EEG data and translate them into efficient controlling signals have generally remained lack of practicality due to the low signal-to-noise ratio of scalp EEG (Abiri et al., 2019; Rashid et al., 2020). The vast majority of EEG-based neurocognitive researches have to rely on the approach of administering a large number of subjects and experimental trials to reveal often subtle neural effects (Boudewyn, Luck, Farrens, & Kappenman, 2018).

In light of the association between cortical activities in actual or imagined movements as shown in the above-mentioned ECoG-based applications, it is reasonable to assume the existence of the association between scalp EEG signals and movements of the effector muscles that control handwriting, albeit with a lower degree. This is the basic assumption underlying our current exploration of decoding handwritten content from scalp level neural signals. Because the scalp EEG is a highly coarse-grained and information-sacrificing filtering of the underlying neural activity on the cortex level (Buzsáki et al., 2012), and is highly susceptible to non-neural artifacts (Pion-Tonachini, Kreutz-Delgado, & Makeig, 2019), the ability to accurately decode handwriting from such noisy data would bear strong merit and significance in the field. The present work was then dedicated to tackling this challenge and pushing the limit in the mapping between scalp EEG and handwritten language production.

The present exploration is grounded on the following two rationales. First, the scalp EEG can be decomposed by advanced blind source separation techniques that restore the temporal

dynamics of independent source generators from the mixed signals (Makeig, Bell, Jung, & Sejnowski, 1996). If different independent sources capture different aspects of handwriting dynamical features, the integration of them would boost the amount of information for classification. Second, the continuous handwriting process is usually constituted by consecutive sub-processes of drawing separate strokes that can be well defined by kinematic features. A single character could be composed of multiple strokes in which each one possesses distinct kinematic features, similar to the sound of a word consisting of multiple syllables. If neural signals are associated with handwriting kinematics, even if weakly, the combinatorial feature of multiple stokes would presumably be able to compensate the low signal-to-noise ratio of EEG and further boost the recognizability of the EEG data in terms of its association with a character or a word. Integrating these features would probably enable the recognition of handwritten characters from scalp EEG with a high accuracy and in an online manner.

2. Methods

2.1 Participant

Five healthy right-handed participants (denoted as P1 – P5) who were native Chinese speakers from mainland China and fluent in English were recruited (3 males, M_{age} = 30.8 (±1.8)). All participants had normal or corrected-to-normal vision and declared no history of mental diseases. The project was approved by the Human Research Ethics Committee (HREC) in the University of Hong Kong. The participants gave their written informed consent before the experiment.

2.2 Instrumentation

The handwriting movements and EEG signals were simultaneously collected at a sampling rate of 60Hz and 1000Hz, respectively. Handwriting trajectories were recorded by a self-developed Android app installed in a tablet (HUAWEI MatePad Pro) equipped with an active stylus with 4096 levels of pressure sensitivity. The app was developed to capture several important events and information during handwriting, including x, y coordinates, timestamp, force, state codes of pen-down (touching the screen), pen-move, and pen-up (leaving the screen) of each single digitalized point of handwritten trajectory. EEG signals were collected with a 32-channel amplifier (BrainAmp, Brain Products GmbH, Germany) referenced to the ground electrode. EEG electrodes were placed on the cap according to the 10-20 international system (Jasper, 1958).

The handwriting trajectories and EEG signals were synchronized by sending time markers of key events in the handwriting stream to the EEG stream. The key events were the first pen-down events of each symbol written in each writing block on the tablet (Figure 1).

2.3 Experiment design

The experiments were conducted in a sound-attenuated room. Participants were required to sit in front of a desk and face squarely to a tablet with a sight distance of approximately 35cm. The tablet was placed in a landscape orientation on an angle-adjustable tablet stand holder with the angle set to 40 degrees above the horizontal plane. The task was to write down each symbol in the sentence "HELLO, WORLD!" (10 block letters and 2 punctuation marks) sequentially on 12 identical blocks on the tablet screen (Figure 1). The participants were required to write the sentence repetitively for 300 times. The app sends a time marker to the EEG stream every time when a writing block detects the first pen-down event. It thus sends 12 markers to the EEG stream during one round of sentence writing after which the written content in the blocks will be erased and the writing and marker-sending processes start over. Participant were instructed to write each symbol in the corresponding block stroke-by-stroke and avoid scribble writing. They can take a break at any time during the task. All participants completed an entire session of this task, i.e., writing the sentences for 300 times. P1 completed an extra session three weeks ago for testing the cross-session accuracy within the same participant. An illustration of a round of writing the sentence was shown in Figure 1 (left).

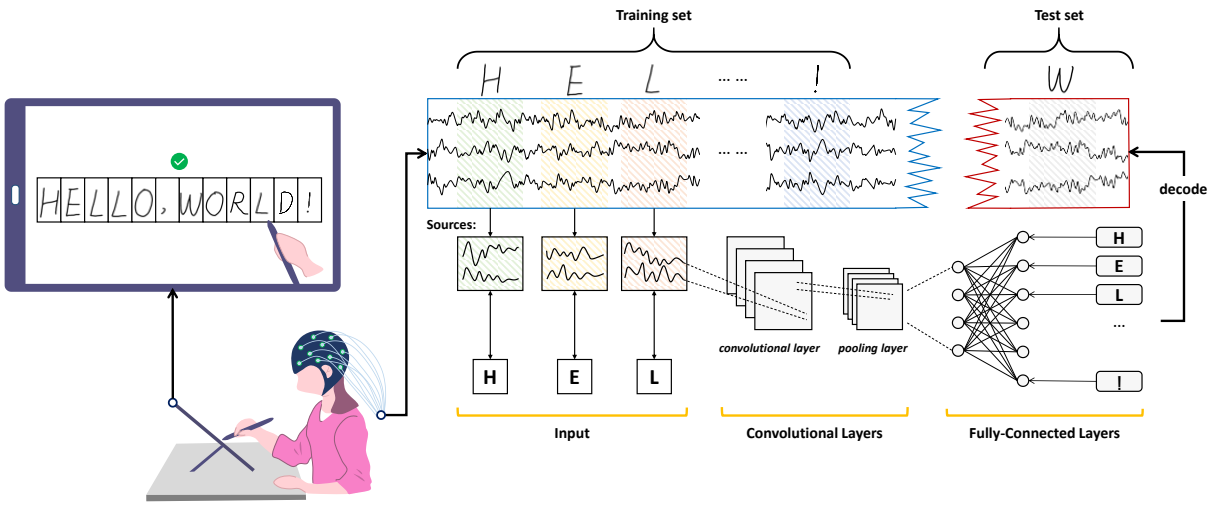

Figure 1. Illustration of the system for learning EEG-handwriting associations and decoding EEG signals.

2.4 Data analysis

The EEG data were preprocessed using MATLAB (version 2020a, The MathWorks) and EEGLAB plugin (Delorme & Makeig, 2004). The data analysis pipeline for machine learning was established as shown in Figure 1 (right). It included: 1) decomposition of raw EEG signals into independent source components; 2) extraction of source signals encompassing the time course of writing each symbol based on markers; 3) partitioning of the data into training and test sets for training and testing the classifier, respectively.

In addition, further analyses were conducted to investigate the neural substrates underpinning the recognition of symbol writing, which included: 1) generating event-related potential (ERP) associated with writing of different symbols; and 2) calculating the cross-correlation between source activities and ongoing handwriting kinematics. The technical details are described below.

2.4.1 Preprocessing and signal decomposition

The entire session of raw EEG data from each participant was first down-sampled to 250Hz and bandpass-filtered at 1-45Hz using a bandpass FIR filter. Next, the EEG segments containing long silence (i.e. no handwriting events recorded for longer than 2 seconds) were truncated. Lastly, independent component analysis (ICA) was applied to decompose the EEG data into independent source activities.

The method ICA is a specific algorithm for implementing blind source separation (BSS). It was selected here because it had demonstrated its success and suitability in decomposing EEG data by its wide applications (Jung et al., 2000). ICA assumes that the EEG signals recorded from the electrodes are linear mixtures of the underlying source activities: $x(t) = \mathbf{A}u(t)$, where x denotes the 2-d matrix of EEG signals, **A** denotes the mixing operation and u denotes the source activities. The sources can be neural or non-neural (e.g. artifacts). The algorithm of ICA is to find an un-mixing matrix **W** such that the unmixed signal $u(t) = \mathbf{W}x(t)$ are statistically independent. The statistical independence was defined by mutual information. Here, the extended algorithm of ICA was used (Lee, Girolami, & Sejnowski, 1999). The ICA algorithm implemented here orders the resultant ICs according to the variance they project to the sensor space (in descending order). The ICs that capture clearly defined sources (e.g., ocular movements, neural processes) are usually ranked in lower orders. ICs ranked in higher orders tend to be noise in nature (Delorme & Makeig, 2004).

2.4.2 Feature extraction

The decomposed source signals encompassing the segments of writing each symbol were used as data features to train the classifier. The raw EEG data from each participant, per session were further processed by the following procedure to extract the relevant features. Firstly, the EEG signals were low-pass filtered at 8Hz, as it was found in the current data that the low frequency bands were more exclusively associated with the movement dynamics, which is also in line with previous finding (Kobler, Sburlea, & Müller-Putz, 2018). Then, the EEG signals were transformed from sensor space to source space using the un-mixing matrix obtained by ICA (see above). Only a subset of the early-ranked ICs (P1-P4: first 8 ICs; P5: first 7 and 10^{th} ICs) were selected to reconstruct the source signals. Next, segments of the reconstructed source signals were taken from the time windows [m_1, m_2] that encompass the first pen-down event (t_j) of writing each symbol, i.e., from m_1 seconds before t_j and m_2 seconds after t_j. Due to individual differences in the handwriting styles, the [m_1, m_2] parameters that led to the best classifier performance for each participant were individual specific (P1: [-1,2]; P2: [-.5,2]; P3: [-1,1.5]; P4: [-1,1.5]; P5: [-.8,2]). It is also worth noting that although optimal performance results were achieved under individually specific time windows, the performance did not show a high degree of sensitivity to the time window parameters (see "Parameter sensitivity below"). Lastly, these data segments and their associated symbols (labels) were then mapped for training and testing the classifier according to the details described in the next section. The data segments were 2-d matrices (resembling a gray-scaled image) with a size of n×m where n is the number of IC selected, and m is determined by the time window parameters m_1 and m_2. The labels were the nine different symbols.

2.4.3 Building of the classifier

The building and training of the CNN network were implemented using the Deep Learning package in MATLAB. The CNN takes a 2-d matrix as input and a 9-unit vector as output. Specifically, the first layer is the input layer; the second layer is a 2-d convolution layer with filter size of 3×3 (padding was added in a way that the output size is equal to the unit size); a batch normalization layer; a rectified linear unit (ReLU) layer; a max pooling layer with a pool size and stride size both equal to 1; a dropout layer with a probability of 0.5; a fully connected layer that transforms the output to the number of labels; a softmax layer and a classification layer that generates the classification output.

Following the general procedure of machine learning, in our application we adopted a simple way that partitioned the dataset into training set and test set. Only the training set was used in the training process and only the test set was used for the accuracy testing, i.e., the test set was not exposed to the classifier during the training process. The training and testing were conducted in three different scenarios as described below, all of which followed the principle that the test set was not exposed to the training process.

1) Within-participant. The purpose of within-participant application was to examine the performance of the classifier trained on an individual in predicting the written symbol from new EEG data immediately generated from the same individual. The classifier was trained on a data segment and tested on another. To more systematically examine how long of handwriting activity would suffice to train a high-accuracy classifier, a stepwise testing of the training outcomes (i.e., accuracy) was performed: in each step, a fix length of initial data segment was used as the training set, and the 500 trials immediately after the training segment was used as the test set. The length of the training set was systematically varied using values of 25, 75, 150, 500, 1000, 1500, 2000, 2500, 3000 trials for each step. The lengths of training set were converted to actual time spent in handwriting for easier understanding. The training and testing were repeated 100 times for each within-participant classifier and the mean and standard deviations of the accuracy results were reported in Figure 3 after removing the outliers out of two folds of inter-quantile range from the 1/4 and 3/4 quantiles.

2) Cross-participant. The purpose of cross-participant application was to examine the performance of the classifier trained on an individual in predicting the written symbol from new EEG data from a different individual. In this scenario, the training and test sets were from the entire session of writing the 300 sentences (but from different individuals). The un-mixing matrix was derived from the training set and applied in the test set to obtain the source activity. Due to the uncertainty of IC polarities, two versions of un-mixing matrice (original and polarity reversed) were applied and the higher accuracy results were obtained. The parameters of m1, m2, and selected ICs were consistent between training and test sets. The training and testing were also repeated 100 times and the means and standard deviations were reported in Figure 4 after removing the outliers out of two folds of inter-quantile range from the 1/4 and 3/4 quantiles.

3) Cross-session. The purpose of cross-session application was to examine the performance of the classifier trained on an individual in predicting the written symbol

from new EEG data from the same individual collected after a long period of time. The participant P1 went through two sessions of data collection separated by three weeks. The cross-session classifier was trained and tested respectively on data segments from P1's two sessions in an implementation way that was the same with the cross-participant scenario.

2.4.4 EEG-based online recognition of handwritten symbols

To test and demonstrate the feasibility of applying the EEG decoder to recognize the handwritten content in an online mode, we built the following pipeline. First, a CNN-based decoder was well trained from participant P1 using sufficient data following the procedure as described above. The ICA decomposition matrix was obtained as well from this training session. Secondly, the raw EEG data were collected online during the handwriting process. The online EEG data was automatically segmented by the event marker generated by the first pen-down event of writing each symbol. The relevant features of this online-collected EEG segment were extracted by ICA decomposition and all the processing as described above. The processed data were then fed to the trained classifier to instantaneously classify and report the result, i.e., instantaneously recognizing what the participant wrote. A video demonstration of the online recognition can be found from supplementary Video 1.

2.4.5 Patterns of neural response associated with symbol writing

Although the machine learning used all contributing source activities (including neural and non-neural ones), it is still worthwhile to examine the neural response patterns associated with the writing of each symbol and how the pattern differs across symbols. To this end, the event-related potentials (ERPs) were calculated after removing the non-neural artifacts. The artifact detection was conducted automatically using MARA algorithm (Winkler, Haufe, & Tangermann, 2011). After detecting and removing the artifacts by ICA and MARA, ERPs were generated associated with each of the nine symbols by averaging the EEG epoch across all trials. The baseline was set to be from 500 ms to 200 ms before the first pen-down event of writing each symbol. The patterns of neural response associated with nine different symbols were shown in Figure 2.

2.4.6 Cross-correlations between EEG and handwriting kinematics signals

To further investigate the major substrates contributing to the EEG-based handwriting recognition, the cross-correlations between two time series—the handwriting kinematics and the ongoing EEG signals—were calculated. For the handwriting kinematics, the velocity at

every time point of handwriting trajectory was calculated based on the formula of dividing the Euclidean distance between two adjacent points by the time interval between them. For EEG signals, the source activities obtained by ICA were used. The reason for using source activities rather than sensor data was that the sources may provide more information regarding which sources activities encode more handwriting kinematics information.

To demonstrate the statistical significance of the cross-correlation, the cross-correlation based on the surrogate EEG data was also calculated. The surrogate EEG data were simply generated by temporally flipping the whole segment of original EEG data. If the cross-correlation from the original data does not stand out from the surrogate data, it would mean that there is not significant association between the handwriting kinematics and EEG signals. The cross-correlations were first calculated separately in each sentence ("HELLO, WORLD!") and the results were averaged across the 300 sentences.

2.4.7 Parameter sensitivity

To examine the parameter sensitivity of the classifier, additional analyses were conducted with respect to three key parameters and settings: time window of the EEG segment encompassing a symbol, number of involved ICs, and type of BSS method used (ICA or principal component analysis (PCA)). For time window, a variety of m1 and m2 parameters were used to cover a large range of time window. Specifically, m1 varied from -1 to -.5 and m2 varied from .5 to 2 with a step of .1. For number of involved ICs, it was systematically varied from 1 to 32 with a step of 1. Note that this operation was based on the order of ICs that was sorted by the variance they contributed to the sensor data. For type of BSS method used, PCA was used as an alternative to the ICA procedure and the performance of both methods were compared at three different situations of component involvement: namely the first 8, 16 and 32 components. Except for the systematically changed parameters as described above, all other parameters and the procedures for building and testing the classifiers remained the same. In the procedure of examining the parameter sensitivity, the first 4/5 portion of the data were used as training set and the last 1/5 portion of data were used as test set. The training and testing were repeated for 5 times and the best performance was recorded.

3. Results

3.1 Variability of EEG pattern across symbols

The ERP patterns corresponding to different symbols were shown in Figure 2. The differences amongst them serve as the foundation for building subsequent machine learning applications.

As shown in Figure 2, the differences in ERP patterns across symbols are visually discernable even after removal of major non-neural artifacts. The patterns of the activation waveforms appear to be somewhat associated with the stroke complexity of the symbols, which supports our assumption that the combinatorial stroke sequences may contribute to the degree of specificity of EEG segments for different symbols. However, the results in Figure 2 were obtained by averaging many trials. Although the foundation was provided, it is not entirely informative regarding whether the differences are largely retained in the noisy single trials or not, which is the key factor affecting the performance of a classifier.

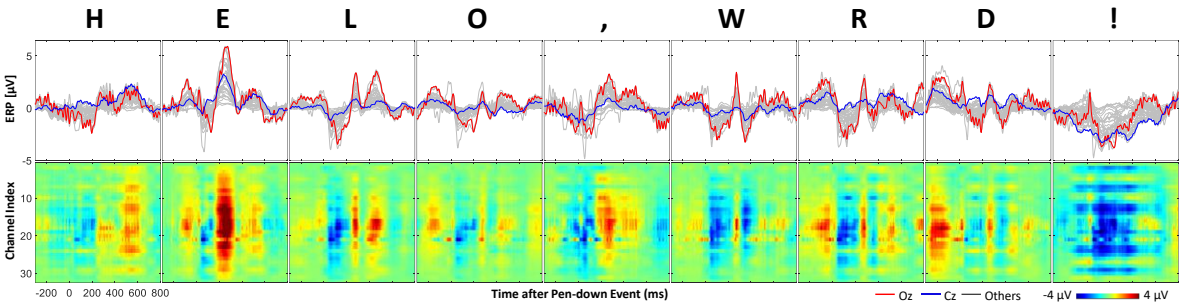

Figure 2. Grand-averaged ERP patterns corresponding to different handwritten symbols. Top: ERP waveforms for all electrodes with Oz and Cz electrodes highlighted in red and blue, respectively. Bottom: The 2-d representations of grand-averaged ERP patterns. They were generated by stacking ERPs from each electrode and using color to represent the amplitude values at each time point.

3.2 Performance of the CNN-based classifier

A CNN-based network was built to classify the two-dimensional EEG patterns as CNN is known to be powerful in capturing key image features in a way that is immune to translational or rotational transformations. This feature is particularly useful in the present case as there exists substantial variabilities in the kinematic features of symbol writing from instance to instance. Because ERP patterns are extremely sensitive to timing, it was expected that great latency variability (translational transformation) existed in the present ERPs from trial to trial, which justified the application of CNN that treats the two-dimensional ERP segments as images. It was further assumed that the signals from the source level possess more discernible information than the sensor level. Due to the difference in the activation strength of different sources, many independent sources could be under-represented at the sensor level, i.e., overwhelmingly covered by strong activation sources. Therefore, directly feeding the activation pattern of independent sources to the training network may lead to more efficient training.

Within-participant: As shown in Figure 3, the classifier reached its full potential after being trained on around 7 minutes of continuous handwriting activity for all participants. It has to be noted here that the accuracy refers to the application on test set (see Method). The full potential for the five participants ranged from 76.8 % (P5) to 97.0 % (P1).

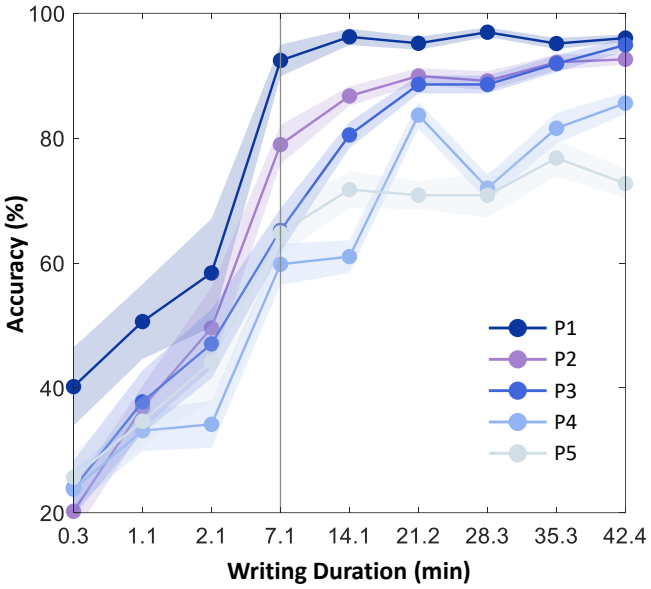

Figure 3. Accuracy of within-participant classifier (applied on test data) as a function of the length of training data. The classifier approached upper limits of accuracy after being trained on around 7 minutes of continuous handwriting. The accuracy at each time point was averaged from 100 realizations. The curves and shadows represent the means and standard deviations.

Cross-participant: The purpose of examining cross-participant classifier was to investigate the commonality and specificity in the EEG-handwriting associations amongst the population. A total of 20 cross-participant applications were conducted. As shown in Figure 4, most of the accuracies were above the chance level (11.1 %). Noticeably, the accuracy between P1 and P3 reached the highest value (around 60 %). The results suggested a high level of both commonalities and specificities in the EEG-handwriting mapping across individuals.

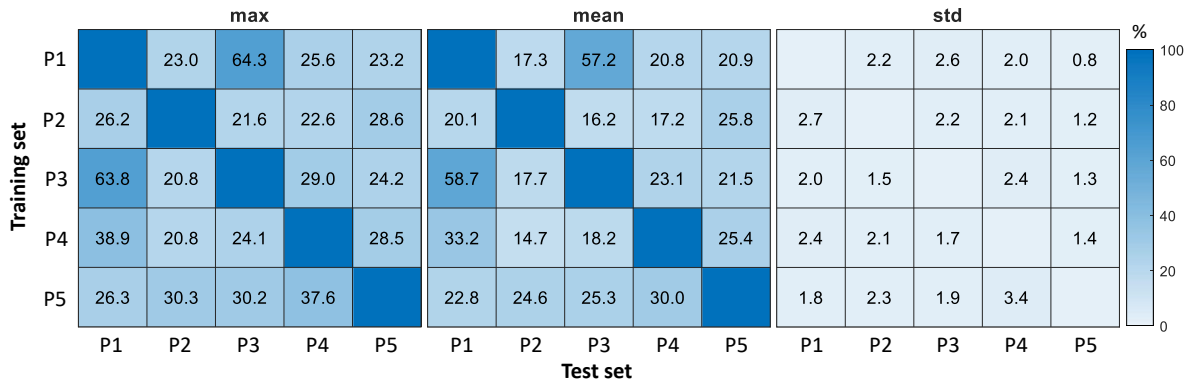

Figure 4. Performance of the classifier in cross-participant application. The results were from 100 realizations. P1-P5 refer to the five participants; 'std' denotes standard deviation.

Cross-session: The cross-session application is the same as the within-participant application except that the training and test sets were separated by three weeks. The participant P1 that showed the highest within-participant accuracy took part in two sessions with three weeks apart. Following the principle that the test set was not exposed to the training session (see Method), the accuracy of this cross-session application is of 87.0%±0.8% (from 100 realizations). This high accuracy indicated the reliability of EEG and handwriting features within a single individual across time.

Demonstration of the online recognition system: The participant P1 took part in another session for demonstrating the classifier's performance in recognizing handwritten content based on EEG data collected online. In this setting, the recognized symbol was directly shown on a computer screen to show the performance of the classifier in real time. A video clip recording the scene of handwriting and online recognition was taped (see Supplementary Video 1).

3.3 Neural substrate underlying the decoding

How did the EEG signals encode the handwriting pattern? One of the potential mechanisms may lie in the neural coding of kinematics and proprioception of the hand movements during handwriting. The profiles of velocity versus time for each symbol possess a high degree of symbol-dependent specificity. To demonstrate that the neural activities measured by scalp EEG are coupled with such kinematic information, the cross-correlation was calculated between the ongoing EEG source activities and the time series of velocities of handwriting. The cross-correlograms (Figure 5) showed strong coupling between the EEG source activities and kinematics streams during handwriting, as seen from source activities that were activated in various areas. The correlations were highly significant and robust across participants.

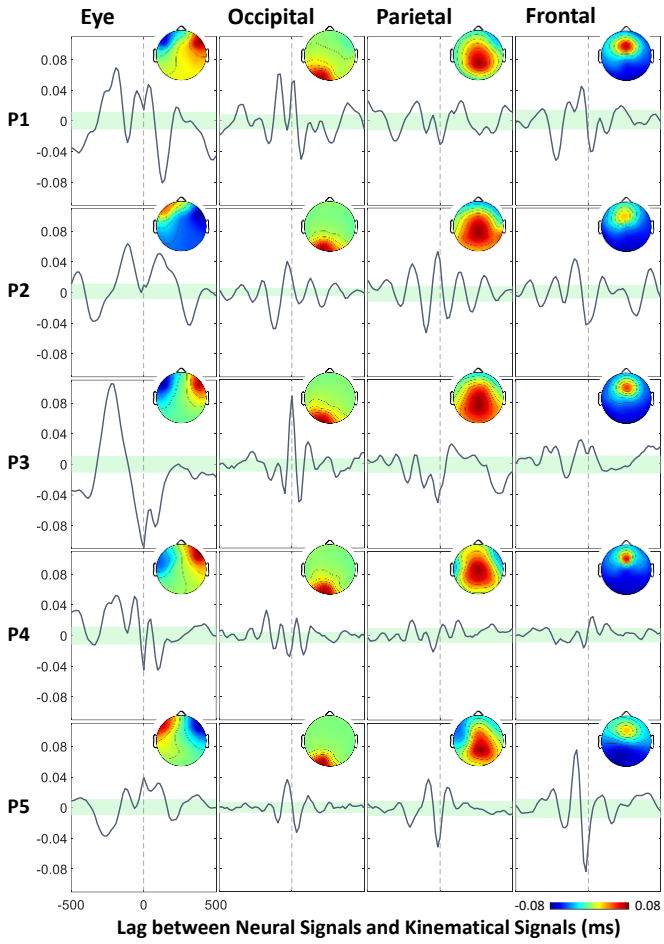

Figure 5. Cross-correlations between EEG source signals and time series of velocity of handwriting movement. Four sources were selected for presenting the association. They are 1) ocular activities, 2) activities in occipital areas, 3) activities in parietal areas, 4) activities in frontal areas of the brain. The upper and lower limits of the cross-correlation calculated from surrogate EEG data were marked in green shadow. The black vertical dashed line denotes zero lag point.

3.4 Parameter sensitivity

As shown in Figure 6, the performance of the classifier was quite robust across a large range of [m1, m2] in all participants. The performance tended to decline when the time window become too narrow, which was expected as less information was fed to the training process. In general, the performance reached asymptote when the time window is wider than [-1s,1s].

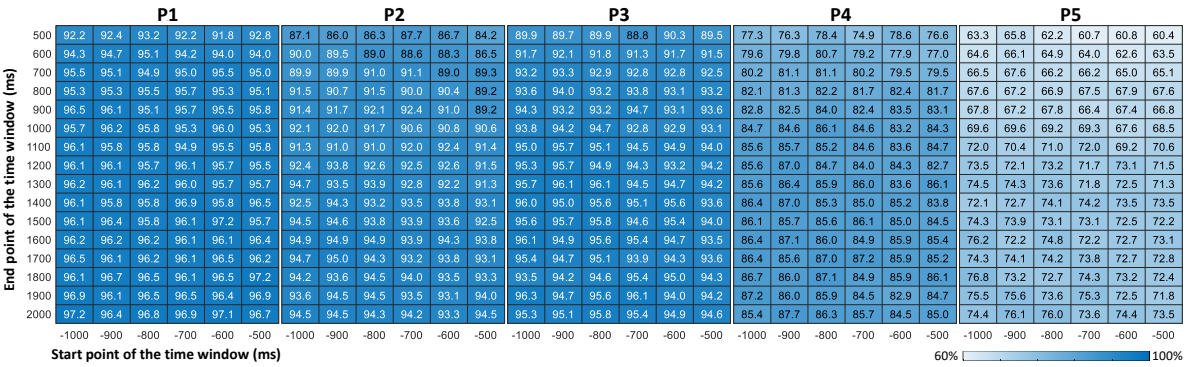

Figure 6. Accuracy of the classifier as a function of time window selected (Chance level: 11.1%).

Figure 7 shows the result of the classifier accuracy as a function of number of ICs involved. The order of the ICs was sorted by the variance they contributed to the sensor data. The result revealed an optimal range of number of ICs involved, roughly from 3 to 15 with an optimum being reached at around 8 ICs. The optimal result was not sensitive to number of ICs involved as demonstrated by the wide flat curve in the middle. However, both involving too few (not enough information provided) or too many (too much noise) components lower the performance.

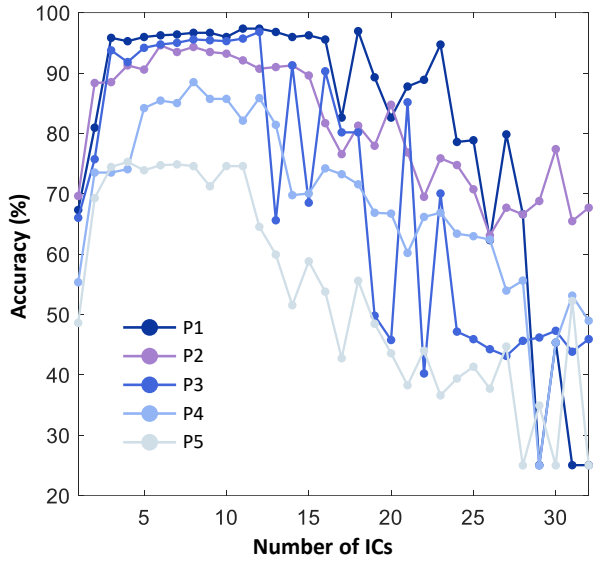

Figure 7. Performance of the classifier as a function of number of ICs (sorted by variance contributed) involved.

In comparison to ICA, PCA performed slightly worse in the present application in the parameter regime in which both methods reached optimal performance (here, using first 8 components). Even though PCA performed better than ICA when all components were involved, the performance in this setting was not good for both methods (see Table 1).

Table 1. The comparison of classifier performance between ICA and PCA.

Num of Comps	P1		P2		P3		P4		P5	
	ICA	PCA	ICA	PCA	ICA	PCA	ICA	PCA	ICA	PCA
8	96.66	96.66	94.31	91.40	95.56	93.20	88.49	84.60	74.58	70.39
16	95.55	59.25	81.69	78.78	90.29	88.21	74.20	63.94	53.77	47.49
32	25.03	40.75	67.68	54.51	45.91	72.40	48.96	61.44	25.00	25.00

Note: 'Num of Comps' refers to the number of ICs/PCs used for classifier training. 'PX' denotes the Participant X. The order of separated components was determined by their variance contributed to sensor data.

4. Discussion

This work presents a CNN-based system demonstrating that handwritten content can be recognized purely from scalp EEG data at a high accuracy. This scalp EEG-based recognition system revealed a very precise mapping between scalp EEG pattern and handwritten content at the semantic level. Although the noisiness of the scalp EEG data does not allow restoration of exact hand movements, it allows restoration of information at higher levels—in the present case, linguistic symbols—that are essential to human's communications.

The key elements that led to the achievement of the system are two-fold: 1) the improvement of feature extraction of scalp EEG by integrating the pattern of independent sources, and 2) the identification of the level of information to be decoded, i.e., focusing on the capsule of kinematic patterns in writing each symbol constituting multiple strokes. The combinatorial features of both elements (independent neural sources, and consecutive strokes) significantly boost the specificity in the mapping between EEG pattern and written information. Accordingly, we expect that script languages with more combinatorial features (e.g., Chinese) would generate a higher performance in the classification.

Our results showed that the cross-individual application did not generate a high accuracy performance. The individual differences in neural and behavioral features still place a challenge in developing a universal classifier to be applied across individuals with a high accuracy. The neural variability can be rooted in various anatomical (e.g., specific organization of sulci and gyri) and physiological (e.g., conductivity of scalp) factors. The behavioral variability can be in handwriting styles (e.g., order of strokes in a symbol). Various factors of inter-individual variability led to the relatively low accuracy in the cross-participant applications in the present work. Future work for improvement in this aspect may resort to collection of larger sample size for training in order to cope with the issue of cross-individual variability in both neural and behavioral features.

Regarding parameter sensitivity, the current classifier system was not sensitive to the key parameters used. In this application, we presented the core results that were based on suitable parameters at which the full potential of the classifier system was reached. The key parameters

and procedures are 1) the time windows surrounding each symbol, 2) selection of independent components (ICs) to be involved and 3) BSS algorithm used. The accuracy results stayed stable across a wide range of time window used both before and after the pen-down. Regarding the involvement of ICs, the performance saturated when around half of the ICs were involved, and became worse when those high-ranked ICs were involved. The current ICA algorithm sorted the ICs according to the variances they contributed to the sensor data. Those high-ranked ICs contributed little variance to the data and tended to be noise-like component, which is why the involvement of them jeopardized the performance. We also compared the performance of using principal component analysis (PCA) as an alternative algorithm of blind source separation. The results showed that it did not outperform the ICA-based classifier.

Although we provided an accurate mapping between scalp EEG patterns and handwritten symbols, it is obvious that this accurate mapping was derived from the process of actual handwriting production, not from imagery of handwriting. One of the major limitations of the current system is that it relies on actual implementation of the action. This imposes a major limitation in the applicability of the current system in BCI applications. Based on foundation of the brain-behavior mapping as shown in the current study, further development that extends to imagery-based paradigm should be done to address the applicability issue. Although imagery-based handwriting recognition system based on cortical activity has shown an excellent performance (Willett et al., 2020), the application on scalp-level signals has not yet been demonstrated. We believe that, by further harnessing the combinatorial features, recognition of mental imagery of handwriting from scalp EEG would be possible, for instance, imagery of the consecutive strokes of Chinese characters—a project that is worth to further explore. The realization of such a system would allow for further development of a mental typing system.

5. Conclusion

Our investigation showed that the mapping between EEG and handwriting dynamics reached a level at which the written symbols can be reliably restored from the EEG data. This result was mainly achieved by exploiting the EEG information at source level and leveraging the combinatorial feature of stroke dynamics during handwriting. Although the current application was still based on actual handwriting, it suggested a novel venue for developing more efficient brain signals-based communications. The era for convenient acquisition of neural signals non-invasively is approaching (Dehais et al., 2019; Kappel, Rank, Toft, Andersen, & Kidmose,

2019). The advancement in the algorithms of feature extraction and machine learning would eventually lead to substantial life enhancement based on instantaneous obtained neural signals.

Acknowledgements This work was supported by the grant from the Hong Kong Research Grant Council (27603818).

References

Abiri, R., Borhani, S., Sellers, E. W., Jiang, Y., & Zhao, X. P. (2019). A comprehensive review of EEG-based brain-computer interface paradigms. *Journal of Neural Engineering, 16*(1). doi:ARTN 011001/10.1088/1741-2552/aaf12e

Aflalo, T., Kellis, S., Klaes, C., Lee, B., Shi, Y., Pejsa, K., . . . Andersen, R. A. (2015). Decoding motor imagery from the posterior parietal cortex of a tetraplegic human. *Science, 348*(6237), 906. doi:10.1126/science.aaa5417

Alimardani, M. (2018). Brain-Computer interface and Motor Imagery Training : The Role of Visual Feedback and Embodiment. In: IntechOpen.

Angrick, M., Herff, C., Mugler, E., Tate, M. C., Slutzky, M. W., Krusienski, D. J., & Schultz, T. (2019). Speech synthesis from ECoG using densely connected 3D convolutional neural networks. *Journal of Neural Engineering, 16*(3). doi:ARTN 036019/10.1088/1741-2552/ab0c59

Anumanchipalli, G. K., Chartier, J., & Chang, E. F. (2019). Speech synthesis from neural decoding of spoken sentences. *Nature, 568*(7753), 493-498. doi:10.1038/s41586-019-1119-1

Boudewyn, M. A., Luck, S. J., Farrens, J. L., & Kappenman, E. S. (2018). How many trials does it take to get a significant ERP effect? It depends. *Psychophysiology, 55*(6), e13049. doi:https://doi.org/10.1111/psyp.13049

Buzsáki, G., Anastassiou, C. A., & Koch, C. (2012). The origin of extracellular fields and currents — EEG, ECoG, LFP and spikes. *Nature Reviews Neuroscience, 13*(6), 407-420. doi:10.1038/nrn3241

Chen, X., Wang, Y., Nakanishi, M., Gao, X., Jung, T.-P., & Gao, S. (2015). High-speed spelling with a noninvasive brain–computer interface. *Proceedings of the National Academy of Sciences, 112*(44), E6058. doi:10.1073/pnas.1508080112

Dehais, F., Duprès, A., Blum, S., Drougard, N., Scannella, S., Roy, R. N., & Lotte, F. (2019). Monitoring Pilot's Mental Workload Using ERPs and Spectral Power with a Six-Dry-Electrode EEG System in Real Flight Conditions. *Sensors, 19*(6), 1324.

Delorme, A., & Makeig, S. (2004). EEGLAB: an open source toolbox for analysis of single-trial EEG dynamics including independent component analysis. *Journal of Neuroscience Methods, 134*(1), 9-21. doi:https://doi.org/10.1016/j.jneumeth.2003.10.009

Fazel-Rezai, R., Allison, B., Guger, C., Sellers, E., Kleih, S., & Kübler, A. (2012). P300 brain computer interface: current challenges and emerging trends. *Frontiers in Neuroengineering, 5*(14). doi:10.3389/fneng.2012.00014

Jasper, H. H. (1958). The ten-twenty electrode system of the International Federation. *Electroencephalography and Clinical Neurophysiology, 10*(2), 370-375. doi:https://doi.org/10.1016/0013-4694(58)90053-1

Jung, T.-P., Makeig, S., Humphries, C., Lee, T.-W., McKeown, M. J., Iragui, V., & Sejnowski, T. J. (2000). Removing electroencephalographic artifacts by blind source separation. *Psychophysiology, 37*(2), 163-178. doi:https://doi.org/10.1111/1469-8986.3720163

Kappel, S. L., Rank, M. L., Toft, H. O., Andersen, M., & Kidmose, P. (2019). Dry-Contact Electrode Ear-EEG. *IEEE Transactions on Biomedical Engineering, 66*(1), 150-158. doi:10.1109/TBME.2018.2835778

Kobler, R. J., Sburlea, A. I., & Müller-Putz, G. R. (2018). Tuning characteristics of low-frequency EEG to positions and velocities in visuomotor and oculomotor tracking tasks. *Scientific Reports, 8*(1), 17713. doi:10.1038/s41598-018-36326-y

Lee, T.-W., Girolami, M., & Sejnowski, T. J. (1999). Independent Component Analysis Using an Extended Infomax Algorithm for Mixed Subgaussian and Supergaussian Sources. *Neural Computation, 11*(2), 417-441. doi:10.1162/089976699300016719

Lotte, F., Bougrain, L., Cichocki, A., Clerc, M., Congedo, M., Rakotomamonjy, A., & Yger, F. (2018). A review of classification algorithms for EEG-based brain-computer interfaces: a 10 year update. *J Neural Eng, 15*(3), 031005. doi:10.1088/1741-2552/aab2f2

Makeig, S., Bell, A. J., Jung, T.-p., & Sejnowski, T. J. (1996). Independent component analysis of electroencephalographic data. In *Advances in Neural Information Processing Systems* (pp. 145-151).

Makin, J. G., Moses, D. A., & Chang, E. F. (2020). Machine translation of cortical activity to text with an encoder–decoder framework. *Nature Neuroscience, 23*(4), 575-582. doi:10.1038/s41593-020-0608-8

Medina-Juliá, M. T., Fernández-Rodríguez, Á., Velasco-Álvarez, F., & Ron-Angevin, R. (2020). P300-Based Brain-Computer Interface Speller: Usability Evaluation of Three Speller Sizes by Severely Motor-Disabled Patients. *Frontiers in Human Neuroscience, 14*(433). doi:10.3389/fnhum.2020.583358

Moses, D. A., Leonard, M. K., & Chang, E. F. (2018). Real-time classification of auditory sentences using evoked cortical activity in humans. *Journal of Neural Engineering, 15*(3). doi:ARTN 036005/10.1088/1741-2552/aaab6f

Padfield, N., Zabalza, J., Zhao, H., Masero, V., & Ren, J. (2019). EEG-Based Brain-Computer Interfaces Using Motor-Imagery: Techniques and Challenges. *Sensors, 19*(6), 1423. Retrieved from https://www.mdpi.com/1424-8220/19/6/1423

Pion-Tonachini, L., Kreutz-Delgado, K., & Makeig, S. (2019). ICLabel: An automated electroencephalographic independent component classifier, dataset, and website. *NeuroImage, 198*, 181-197. doi:https://doi.org/10.1016/j.neuroimage.2019.05.026

Rashid, M., Sulaiman, N., P. P. Abdul Majeed, A., Musa, R. M., Ab. Nasir, A. F., Bari, B. S., & Khatun, S. (2020). Current Status, Challenges, and Possible Solutions of EEG-Based Brain-Computer Interface: A Comprehensive Review. *Frontiers in Neurorobotics, 14*(25). doi:10.3389/fnbot.2020.00025

Sun, P., Anumanchipalli, G. K., & Chang, E. F. (2020). Brain2Char: a deep architecture for decoding text from brain recordings. *Journal of Neural Engineering*. doi:10.1088/1741-2552/abc742

Willett, F. R., Avansino, D. T., Hochberg, L. R., Henderson, J. M., & Shenoy, K. V. (2020). High-performance brain-to-text communication via imagined handwriting. *bioRxiv*.

Wilson, G. H., Stavisky, S. D., Willett, F. R., Avansino, D. T., Kelemen, J. N., Hochberg, L. R., . . . Shenoy, K. V. (2020). Decoding spoken English from intracortical electrode arrays in dorsal precentral gyrus. *Journal of Neural Engineering, 17*(6). doi:ARTN 066007/10.1088/1741-2552/abbfef

Winkler, I., Haufe, S., & Tangermann, M. (2011). Automatic Classification of Artifactual ICA-Components for Artifact Removal in EEG Signals. *Behavioral and Brain Functions, 7*(1), 30. doi:10.1186/1744-9081-7-30

Zhang, W., Tan, C., Sun, F., Wu, H., & Zhang, B. (2018). A Review of EEG-Based Brain-Computer Interface Systems Design. *Brain Science Advances, 4*(2), 156-167. doi:10.26599/bsa.2018.9050010